Quantitative predictions of maximum strain storage in shape memory polymers (SMP)

Hornat, Chris C.; Nijemeisland, Marlies; Senardi, Michele; Yang, Ying; Pattyn, Christian; van der Zwaag, Sybrand; Urban, Marek W.

DOI
10.1016/j.polymer.2019.122006

Publication date
2020

Document Version
Final published version

Published in
Polymer

Citation (APA)
Hornat, C. C., Nijemeisland, M., Senardi, M., Yang, Y., Pattyn, C., van der Zwaag, S., & Urban, M. W. (2020). Quantitative predictions of maximum strain storage in shape memory polymers (SMP). *Polymer*, *186*, Article 122006. https://doi.org/10.1016/j.polymer.2019.122006

Polymer 186 (2020) 122006

Contents lists available at ScienceDirect

Polymer

journal homepage: http://www.elsevier.com/locate/polymer

Short communication

Quantitative predictions of maximum strain storage in shape memory polymers (SMP)

Chris C. Hornat [a], Marlies Nijemeisland [b], Michele Senardi [b], Ying Yang [a], Christian Pattyn [a], Sybrand van der Zwaag [b,**], Marek W. Urban [a,*]

[a] Department of Materials Science and Engineering, Center for Optical Materials Science and Engineering Technologies (COMSET), Clemson University, Clemson, SC, 29634, USA

[b] Novel Aerospace Materials Group, Faculty of Aerospace Engineering, Delft University of Technology, Kluyverweg 1, Delft, HS, 2629, the Netherlands

ARTICLE INFO

Keywords:
Shape memory
Polymers
Quantitative determination

ABSTRACT

Shape memory polymers (SMPs) are dynamic materials able to recover previously defined shapes when activated by external stimuli. The most common stimulus is thermal energy applied near thermal transitions in polymers, such as glass transition (T_g) and melting (T_m) temperatures. The magnitude of the geometrical changes as well as the amount of force and energy that a SMP can output are critical properties for many applications. While typically deformation steps in the shape memory cycles (SMC) are performed at temperatures well above thermal transitions used to activate shape changes, significantly greater amounts of strain, stress, and mechanical energy can be stored in T_g-based SMPs when deformed near their T_g. Since maximum shape memory storage capacity can be appraised by evaluating the viscoelastic length transitions (VLTs) in a single dynamic mechanical analysis (DMA) experiment, this study correlates VLTs with the measured storage capacities obtained from stress-strain experiments for a broad range of well-defined crosslinked acrylates, epoxies, and polyurethanes. This systematic approach allows for assessment of crosslink/junction density (ν_j), viscoelasticity, and chemical composition effects on maximum deformability, and enables predictions of the magnitude of shape memory properties across a wide variety of polymers. These studies demonstrate that the maximum storable strain ($\varepsilon\text{-store}_{max}$) can be accurately predicted using junction density (ν_j) and shape memory factor (SMF), the latter accounting for the contribution of chemical makeup.

Shape memory polymers (SMPs) represent a class of materials capable of recovering internally stored shapes from temporarily fixed geometrical arrangements when triggered by the application of proper stimuli [1–4]. Thermal energy is the most common stimulus, although polymers and composites exhibiting shape changes triggered by light [5–7], chemical redox [8], electric current [9,10], alternating magnetic fields [11–13], high intensity ultrasound [14], and exposure to water [15–17] (vapor or liquid) or other solvents [18] have been developed as well. Numerous applications have emerged from these studies, ranging from self-tightening wound sutures [19], to self-expanding stents [20], complex 4D printed structures and devices [21,22], pumps and valves for microfluidics [23], smart textiles with temperature dependent moisture permeability [24], reversible dry adhesives [25,26], self-deployable structures for aerospace [27], soft robots [28], and self-repairing materials [29–32]. For many of these and other applications SMP performance is determined by the magnitude of shape changes and/or how much force/work can be output. Therefore, knowledge about the amount of strain, stress, and mechanical energy that SMPs can store is highly desirable. In view of these considerations, the ability to predict maximum storage capacities is of great scientific interest and technological importance.

For thermal SMPs, most commonly the deformation step during which the strain, stress, and energy are stored is performed in the rubbery plateau region, well above the reversible switching temperature, such as the glass transition temperature (T_g). Considering that for crosslinked amorphous SMPs the maximum storable strain ($\varepsilon\text{-store}_{max}$) is determined by their failure strains [33], under these conditions the storage capacities are typically governed by crosslink density [34]. Since polymers exhibit enhanced deformability in the T_g-region, increased storage of strain, stress, and entropic energy are enabled as a result of

* Corresponding author.
** Corresponding author.
E-mail addresses: S.vanderZwaag@tudelft.nl (S. van der Zwaag), mareku@clemson.edu (M.W. Urban).

https://doi.org/10.1016/j.polymer.2019.122006
Received 2 September 2019; Received in revised form 30 October 2019; Accepted 14 November 2019
Available online 14 November 2019

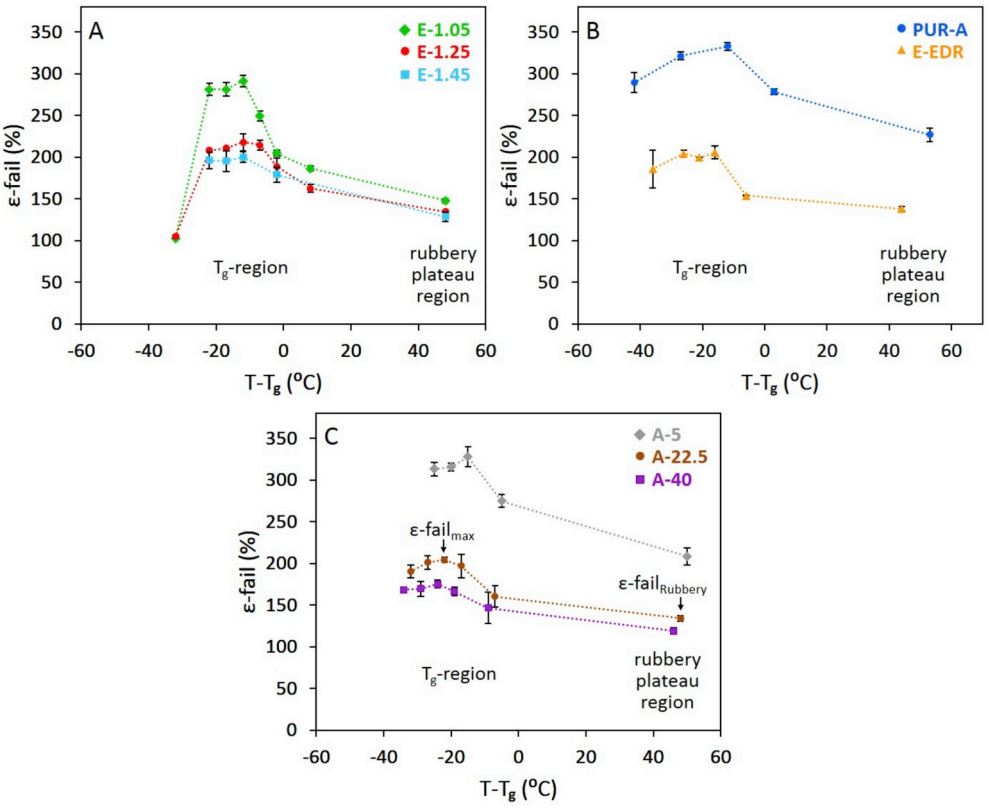

Fig. 1. Tensile failure strain plotted as a function of temperature relative to T_g for (A) E−1.05, E−1.25, E−1.45, (B) E-EDR, and PUR-A, (C) A-5, A-22.5, A-40 (where $T_g = T\tan\delta_{max}$ from DMA, and the strain rate during tensile testing was 10%/min).

Table 1
Shape memory factor (SMF) for each material determined from $\varepsilon\text{-fail}_{rubbery}$ data (Figure S1, B and C).

Specimen	Shape Memory Factor (SMF)
A-5	0.998
A-22.5	0.985
A-40	0.953
E−1.05	1.009
E−1.25	1.023
E−1.45	1.029
E-EDR	1.003
PUR-A	1.512

"viscoelastic toughening." [33,35,36] Attributed to the increased "viscous-like" nature of polymers in the T_g-region, energy dissipation measured as mechanical hysteresis allows for larger deformations prior to rupture [37–40]. Although this concept is qualitatively known for a few selected polymers that have been investigated, a general relationship in a universal quantitative sense across various polymer chemistries has not been established. Means to predict maximum storable strain as well as stress and energy for SMPs are critical for future technological advances.

Recent studies showed that polymers display unique shape memory transitions referred to as viscoelastic length transitions (VLTs) near their T_g which can be measured in a single dynamic mechanical analysis (DMA) experiment, where directional elongations and subsequent retractions are observed due to release of stored entropic energy [41]. The concept takes into account junction density as well as viscous-like components of polymer networks and by combining viscoelastic theory and rubber elasticity allows predictions of shape memory effects. The extension is a result of "viscous-like" behavior of the network at the onset of the T_g, while the retraction is driven by conformational entropy due to chemical/physical crosslinks and/or chain entanglements. Quantifying VLTs in terms of maximum stored strain (ε_{max}), stress (σ_{SF} at ε_{max}), and entropic energy density (ΔS_S), which combines stress and strain aspects, allowing estimates of relative shape memory capacity. Although the VLT is not directly related to the elastic-viscous transition of tear fracture of rubber, both are related to and associated with viscoelasticity and viscoelastic changes.

In order to predict the maximum shape memory storage capacity quantitatively, these studies are driven by the hypothesis that crosslink/junction density (ν_j) and viscoelastic responses account for the enhanced deformability near the T_g-region, which enables larger shape changes. To test this hypothesis, several chemically different crosslinked acrylate-, epoxy-, and urethane-based polymers were synthesized with a broad range of ν_j values and viscoelastic properties. Combining DMA and tensile stress-strain experiments across their T_g-regions this study illustrates the development of quantitative assessments and determination of absolute maximum shape memory storage capacity in crosslinked amorphous SMPs.

As pointed out above, recent studies showed that dynamic and static forces during DMA can be utilized to make relative quantitative assessments of storage capacities in T_g-based SMPs through VLTs [41]. It was demonstrated that the magnitude of VLT maximum stored strain (ε_{max}), stress (σ_{SF} at ε_{max}), and entropic energy density (ΔS_S) are determined by junction density (ν_j) and viscoelastic behavior ($\tan\delta_{max}$). This study aims to correlate VLT values from DMA measurements and storage capacities obtained from stress-strain experiments at appropriate temperatures, with the objective to establish the fundamental effects of ν_j, viscoelasticity, and chemical makeup, on the deformability of non-crystalizing thermosets. For that reason, several well-defined crosslinked acrylates (A-5, A-22.5, A-40), epoxies (E−1.05, E−1.25, E−1.45, E-EDR), and polyurethanes (PUR-A) were prepared, representing both aliphatic (acrylates and polyurethane) and aromatic

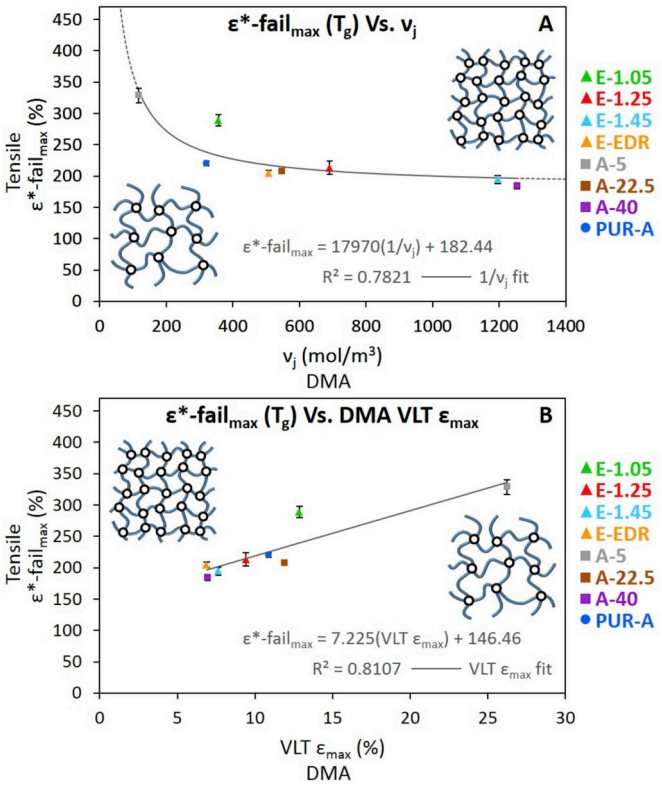

Fig. 2. Maximum failure strain normalized for chemical makeup (ε*-fail$_{max}$) from tensile experiments as a function of (A) ν_j (ν_j from E'$_R$ in DMA) and (B) VLT maximum strain (ε_{max}) from DMA for A-5, A-22.5, A-40, E−1.05, E−1.25, E−1.45, E-EDR, and PUR-A. Normalization factors (SMFs) are shown in Table 1. Dashed line represents extrapolation of trend line beyond the range of experimental ν_j values.

(epoxies) structures. Details regarding their preparation are provided in the Experimental Section, and molar ratios as well as rubbery moduli values are summarized in Table S1.

To determine the largest strain a SMP is capable of storing (ε-store$_{max}$), it is necessary to identify its maximum failure strain (ε-fail$_{max}$), which occurs in the T$_g$-region. Fig. 1 illustrates tensile failure strain (ε-fail) as a function of temperature across the respective T$_g$s and rubbery plateau temperature regions. As anticipated, for each polymer the failure strains in the T$_g$-regions are larger than in the rubbery plateaus (ε-fail$_{Rubbery}$), confirming that more strain can be stored in SMPs when deformed near T$_g$ rather than in the rubbery plateau region as conventionally done in prior studies.

In order to account for chemical composition on ε-store$_{max}$, shape memory factor (SMF) is introduced, and its value for each polymer are listed in Table 1. Defined as the ratio of measured ε-fail$_{Rubbery}$ for each polymer to its expected value (based on $1/\nu_j$ fit), SMF is expressed as T$_g$

$$\text{SMF} = \frac{\varepsilon\text{-fail}_{Rubbery}}{A\left(\frac{1}{\nu_j}\right) + B} \quad (1)$$

where: A and B are fitting parameters, when fitting ε-fail$_{Rubbery}$ values against inverse junction density. SMF characterizes chemical contributions to shape memory storage capacity and it is a universal tool enabling comparison across all polymer chemistries.

Higher SMF values signify greater enhancement of shape memory storage capacities relative to ν_j. All acrylates and epoxies show nearly the same SMFs ~1, indicating minimal effect of chemical composition on their shape memory behavior, but the SMF of PUR-A is considerably higher (SMF = 1.512). The latter is likely attributable to interchain attractive forces resulting from hydrogen bonding [42], allowing greater deformation prior to rupture [43]. The presence of secondary inter-chain interactions may contribute to shape memory storage capacities when interchain attractive forces in non-crystalizing thermosets are present, thus enabling considerable shape memory enhancements.

As the concept of the SMF aims to account for chemical effects on ε-store$_{max}$, the relationship between ε-fail$_{max}$ and ν_j was determined independently of chemical structure. This normalization was accomplished by taking the ratio of ε-fail$_{max}$ to SMF (ε*-fail$_{max}$ = ε-fail$_{max}$/SMF) for each polymer. Fig. 2, A shows that normalized maximum failure strain (ε*-fail$_{max}$) is inversely proportional to ν_j. Thus, SMP networks with lower ν_j values exhibit greater maximum deformability and consequentially are able to store more strain. Recalling that stored VLT ε_{max} is inversely related to ν_j as well [41], Fig. 2, B illustrates the direct relationship between VLT ε_{max} obtained from DMA results and ε*-fail$_{max}$ from tensile measurements. This reiterates the significance of VLTs to shape memory properties and validates their quantitative predictions of shape memory behavior. Inserts in Fig. 2A and B visually depict trends between network densities and the resulting ε*-fail$_{max}$ and VLT ε_{max} values.

To verify the relationships for VLTs, Fig. 3 plots VLT ε_{max}, σ_{SF} at ε_{max}, and ΔS_S values as a function of ν_j and tan δ_{max}. As shown, VLT ε_{max} is inversely related to ν_j and proportional to tan δ_{max} (Fig. 3, A), while VLT σ_{SF} at ε_{max} is an increasing function of both ν_j and tan δ_{max} (3, B). These results indicate that during VLTs polymers store both more strain and stress as "viscous-like" response increases (higher tan δ_{max}), whereas lower ν_j values result in greater elongation but lower stored stress. Since area under a stress-strain curve is proportional to the deformation energy, VLT ΔS_S is proportional to the product of VLT ε_{max} and σ_{SF} at ε_{max} (Fig. 3C and D) in the DMA experiment as well. Thus, the shape memory effect (SME) can be viewed as a continuous function ranging from low strain-high stress networks to high strain-low stress networks over which high energy storage can potentially be achieved. Table S2 of the Supporting Documents summarizes the DMA results.

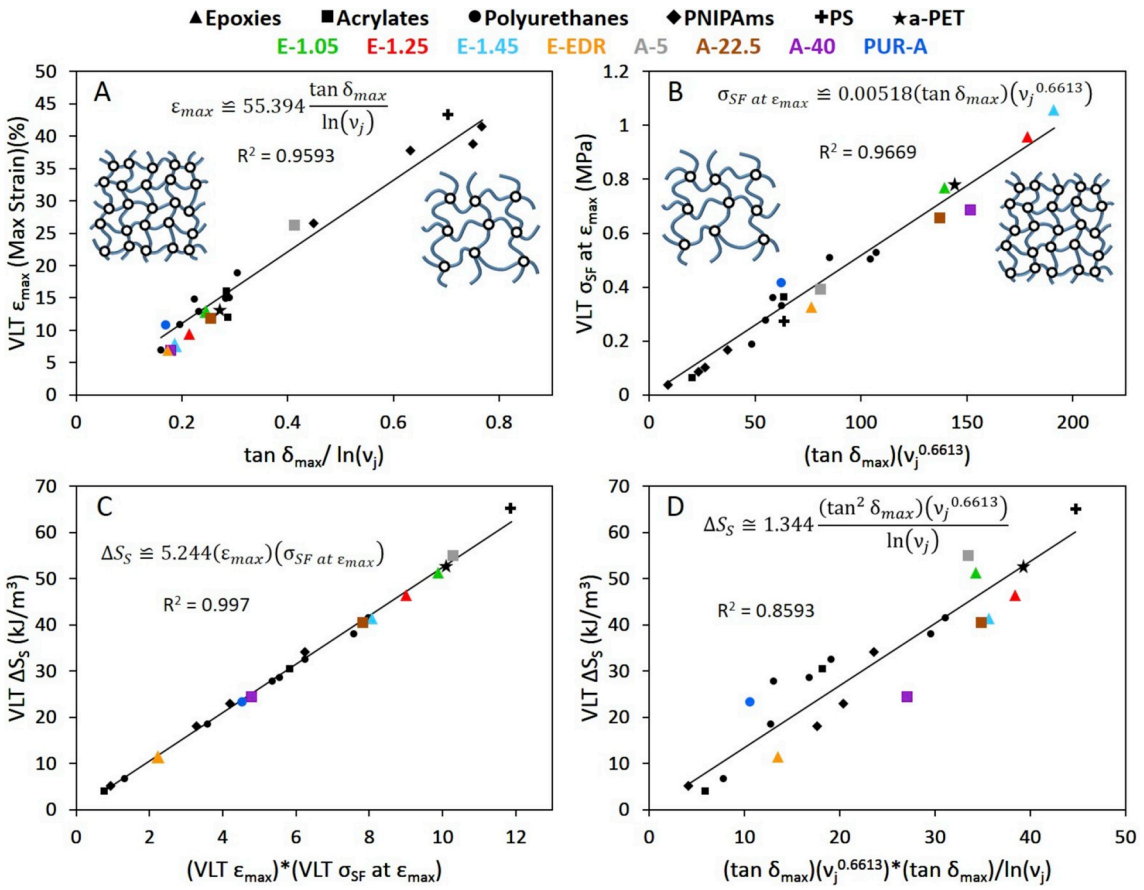

Fig. 3. Plots of VLT (A) strain (ε_{max}), (B) stress (σ_{SF} at ε_{max}), and (D) stored entropic energy density (ΔS_S) from DMA experiments as functions of junction density (ν_j) and tan δ_{max}. (C) Calculated VLT ΔS_S plotted against measured VLT strain (ε_{max}) and stress (σ_{SF} at ε_{max}) from the DMA experiments. Data points in black come from previous studies [41] while A-5, A-22.5, A-40, E−1.05, E−1.25, E−1.45, E-EDR, and PUR-A are identified in colors indicated in the legend above the plots. (For interpretation of the references to color in this figure legend, the reader is referred to the Web version of this article.)

These studies show that crosslink/junction density (ν_j) is the primary determining factor of ε-fail$_{max}$ and thus ε-store$_{max}$ for an SMP. The viscoelastic changes/viscous resistance around T_g that results in increased energy dissipation to delay crack formation/growth and propagation [38–40] appear to be similar for different polymer chemistries. At temperatures below T_g, ε-fail decreases as a result of the decreasing molecular mobility and increased relaxation time, hindering long-range molecular motions in the time scale of the experiment. As temperature increases above T_g, ε-fail decreases as a result of decreasing energy dissipation as free volume increases. VLT ε_{max} provides an equivalently accurate prediction of ε-fail$_{max}$ as ν_j, verifying its importance and relationship to shape memory and viscoelastic properties. Chemical makeup may play a role in cases of specific additional interchain attractive forces, such as hydrogen bonding, expressed by shape memory factor (SMF). Furthermore, it should be emphasized that the critical factors dictating maximum failure strain in amorphous polymers are (1) junction density and (2) viscoelasticity which both contribute to DMA and tensile measurements. In particular, VLT maximum strain (DMA) and maximum tensile failure strain (static stress-strain) increase as junction/crosslink density decreases, and both occur in the Tg-region where polymers exhibit pronounced viscoelastic behavior.

Acknowledgments

The authors (CCH and MWU) thank the National Science Foundation for supporting this research under the award DMR 1744306 and partially by the J.E. Sirrine Foundation Endowment at Clemson University.

Appendix A. Supplementary data

Supplementary data to this article can be found online at https://doi.org/10.1016/j.polymer.2019.122006.

References

[1] A. Lendlein, S. Kelch, Angew. Chem. Int. Ed. 41 (2002) 2034.
[2] C. Liu, H. Qin, P.T. Mather, J. Mater. Chem. 17 (2007) 1543.
[3] T. Xie, Polymer 52 (2011) 4985.
[4] G.J. Berg, M.K. McBride, C. Wang, C.N. Bowman, Polymer 55 (2014) 5849.
[5] A. Lendlein, H. Jiang, O. Jünger, R. Langer, Nature 434 (2005) 879.
[6] J.R. Kumpfer, S.J. Rowan, J. Am. Chem. Soc. 133 (2011) 12866.
[7] K.M. Lee, H. Koerner, R.A. Vaia, T.J. Bunning, T.J. White, Soft Matter 7 (2011) 4318.
[8] D. Aoki, Y. Teramoto, Y. Nishio, Biomacromolecules 8 (2007) 3749.
[9] J.W. Cho, J.W. Kim, Y.C. Jung, N.S. Goo, Macromol. Rapid Commun. 26 (2005) 412.
[10] H. Koerner, G. Price, N.A. Pearce, M. Alexander, R.A. Vaia, Nat. Mater. 3 (2004) 115.
[11] R. Mohr, K. Kratz, T. Weigel, M. Lucka-Gabor, M. Moneke, A. Lendlein, Proc. Natl. Acad. Sci. U.S.A. 103 (2006) 3540.
[12] A.M. Schmidt, Macromol. Rapid Commun. 27 (2006) 1168.
[13] C.M. Yakacki, N.S. Satarkar, K. Gall, R. Likos, J.Z. Hilt, J. Appl. Polym. Sci. 112 (2009) 3166.
[14] G. Li, G. Fei, H. Xia, J. Han, Y. Zhao, J. Mater. Chem. 22 (2012) 7692.
[15] B. Yang, W.M. Huang, C. Li, C.M. Lee, L. Li, Smart Mater. Struct. 13 (2003) 191.
[16] W.M. Huang, B. Yang, L. An, C. Li, Y.S. Chan, Appl. Phys. Lett. 86 (2005) 114105.
[17] X. Qi, X. Yao, S. Deng, T. Zhou, Q. Fu, J. Mater. Chem. 2 (2014) 2240.
[18] H. Lv, J. Leng, Y. Liu, S. Du, Adv. Eng. Mater. 10 (2008) 592.
[19] A. Lendlein, R. Langer, Science 296 (2002) 1673.
[20] K. Gall, C.M. Yakacki, Y. Liu, R. Shandas, N. Willett, K.S. Anseth, J. Biomed. Mater. Res. A 73 (2005) 339.
[21] Q. Ge, A.H. Sakhaei, H. Lee, C.K. Dunn, N.X. Fang, M.L. Dunn, Sci. Rep. 6 (2016) 31110.

[22] L. Huang, R. Jiang, J. Wu, J. Song, H. Bai, B. Li, Q. Zhao, T. Xie, Adv. Mater. 29 (2017) 1605390.
[23] M. Ebara, K. Uto, N. Idota, J.M. Hoffman, T. Aoyagi, Soft Matter 9 (2013) 3074.
[24] S. Mondal, J. L. Hu, 2006.
[25] S. Reddy, E. Arzt, A. del Campo, Adv. Mater. 19 (2007) 3833.
[26] T. Xie, X. Xiao, Chem. Mater. 20 (2008) 2866.
[27] W.M. Sokolowski, S.C. Tan, J. Spacecr. Rocket. 44 (2007) 750.
[28] B. Jin, H. Song, R. Jiang, J. Song, Q. Zhao, T. Xie, Sci. Adv. 4 (2018), eaao3865.
[29] X. Xiao, T. Xie, Y.-T. Cheng, J. Mater. Chem. 20 (2010) 3508.
[30] E.D. Rodriguez, X. Luo, P.T. Mather, ACS Appl. Mater. Interfaces 3 (2011) 152.
[31] X. Luo, P.T. Mather, ACS Macro Lett. 2 (2013) 152.
[32] Y. Yang, D. Davydovich, C.C. Hornat, X. Liu, M.W. Urban, Chem 4 (2018) 1928–1936.
[33] C.M. Yakacki, S. Willis, C. Luders, K. Gall, Adv. Eng. Mater. 10 (2008) 112.
[34] A.M. Ortega, S.E. Kasprzak, C.M. Yakacki, J. Diani, A.R. Greenberg, K. Gall, J. Appl. Polym. Sci. 110 (2008) 1559.
[35] D.L. Safranski, K. Gall, Polymer 49 (2008) 4446.
[36] K.E. Smith, J.S. Temenoff, K. Gall, J. Appl. Polym. Sci. 114 (2009) 2711.
[37] T.L. Smith, J. Polym. Sci. A Polym. Chem. 32 (1958) 99.
[38] E.H. Andrews, J. Mech. Phys. Solids 11 (1963) 231.
[39] J.A.C. Harwood, A.R. Payne, J. Appl. Polym. Sci. 12 (1968) 889.
[40] T.L. Smith, Polym. Eng. Sci. 17 (1977) 129.
[41] C.C. Hornat, Y. Yang, M.W. Urban, Adv. Mater. 29 (2017).
[42] M.M. Coleman, K.H. Lee, D.J. Skrovanek, P.C. Painter, Macromolecules 19 (1986) 2149.
[43] T.L. Smith, Strength and extensibility of elastomers, in: Rheology, Elsevier, 1969, p. 127.